Supporting Information

Robust and Conductive Red $MoSe_2$ for Stable and Fast Lithium Storage

Sanpei Zhang,[†,‡] Gan Wang,[†,‡] Jun Jin,[†] Linlin Zhang[†], Zhaoyin Wen[†,] and Jianhua Yang,[†]*

[†] *CAS Key Laboratory of Materials for Energy Conversion, Shanghai Institute of Ceramics, Chinese Academy of Sciences, Shanghai 200050, P. R. China*

E-mail: zywen@mail.sic.ac.cn

[‡] *University of Chinese Academy of Sciences, Beijing 100049, P. R. China*

Content

1. Experimental Section

2. UV–visible absorption spectra of the prepared series red $MoSe_2$ samples

3. XRD, SEM and TEM images of the prepared MoO_3 nanosheets

4. SEM and TEM images of the prepared pure $MoSe_2$ nanosheets

5. EDX spectra of the red $MoSe_2$ nanosheets

6. Elemental mapping images of the red $MoSe_2$ nanosheets.

7. I-V curves of all the samples

8. The electronic conductivity of the prepared series red $MoSe_2$ samples

9. XPS spectra of the red $MoSe_2$ nanosheets.

10. XPS spectra of the red MoO_3 nanosheets

11. BET analysis results of the black $MoSe_2$ and red $MoSe_2$ nanosheets

12. Discharge-charge voltage profiles of the Li-ion batteries with black $MoSe_2$ anode

13. Discharge-charge voltage profiles of the Li-ion batteries with MoO_3 electrode.

14. CV profiles of red $MoSe_2$ anode

15. Rate capability of the red $MoSe_2$ anode

1. Experimental Section

Samples Preparation

Hexaammonium heptamolybdate tetrahydrate ($(NH_4)_6Mo_7O_{24}\cdot 4H_2O$), thiourea ($NH_2CSNH_2$) and selenourea ($NH_2CSeNH_2$) were purchased from the Sigma-Aldrich Company. The autoclave (model number 4749) was ordered from the Nanjing RNK Science and tech Company.

Preparation of pure $MoSe_2$: The synthesis of the $MoSe_2$ nanosheets was conducted in pure N_2 atmosphere environment. Firstly, 7 mmol NH_2CSeNH_2 was dissolved in 30 mL deionized water under vigorous stirring for 30 min to form a homogeneous solution. Then 1 mmol $(NH_4)_6Mo_7O_{24}\cdot 4H_2O$ was added into the solution and stirred for 1 h. Subsequently, the solution was transferred into a 43 mL Teflon-lined stainless-steel autoclave and kept at 230°C for 20 h. After being cooled to room temperature, the generated precipitates were filtered and washed with ethanol and water. The precipitates separated from the solution by centrifugation were freeze dried for 24 h.

Preparation of Red $MoSe_2$: Red $MoSe_2$ nanosheets were synthesized by a fast-oxidized process. Specifically, pure $MoSe_2$ nanosheets and potassium permanganate powders were separately placed in a two-zone tube furnace, which was evacuated until the pressure was lower than 5 Pa. The zone containing $MoSe_2$ nanosheets was next heated to 250-350°C, and the zone containing potassium permanganate to 500°C, then held for 1 h. Red $MoSe_2$ nanosheets were obtained after cooling to the ambient temperature. In comparison, the red $MoSe_2$ prepared with different annealing time was synthesized by the same procedure.

Structural Analyses

Ultraviolet–visible (UV–vis) absorption spectroscopy analysis in the wavelength range of 250–1000 nm is completed by using a Hitachi UV-4100 spectrophotometer. XRD was conducted on a Rigaku D/Max ultima II with Cu Kα radiation. The FESEM images were taken on a JEOL JSM-6700F SEM. TEM images were taken on JEOL JEM-2100F microscopes. X-ray photoelectron spectroscopy analysis was conducted

using a twin anode gun, Mg KR (1253.6 eV) (Microlab 310F Scanning Auger Microprobe, VG Scientific Ltd.). The specific surface area was further measured by the Brunauer–Emmett–Teller (BET) method using nitrogen adsorption–desorption isotherms on a Micromeritics Tristar II 3020 analyzer. The discharge products were analyzed by X-ray photoelectron spectroscopy (ESCALAB 250). The room-temperature *I–V* characteristics were carried out in the voltage range of -1 V–+1 V at a scanning rate of 1 mV/s.

Electrochemical measurements

Lithium-ion batteries: active material (70 wt.%), Ketjen Black (KB) carbon (EC600JD) (20 wt.%) and Polytetrafluoroethylene (PTFE) binder (10 wt. %, Aldrich) in ethanol were mixed into a homogeneous slurry. The obtained slurry was pasted on stainless steel mesh, followed by drying in a vacuum oven for 12 hours at 80 ˚C. After cutting the electrode disks of 1.0 cm diameter, the disk was used as the anode of LIBs without calendared before testing and the average thickness of the coating is ~ 0.02 mm. The cells were assembled in an argon-filled glove box (O_2 ⩽ 0.1 ppm, H_2O ⩽ 0.1 ppm) with the prepared anode as working electrode and lithium metal foil as the counter/reference electrode. The electrolyte is 1M $LiPF_6$ in a mixture of ethylene carbonate and diethyl carbonate (1:1 by weight). Glass fiber (Whatman) was used as separator. The typical mass loading of active materials is about 0.8 mg cm^{-2}. The charge-discharge tests were performed on a LAND battery tester. Cyclic voltammograms (CV) were obtained on a CHI 660D electrochemical workstation. For ex-situ XPS and HRTEM at different reactive potentials, the electrode sheets cycled at a current density of 500 mA/g were required to be removed from the disassembled batteries and washed with DMC.

2. UV–visible absorption spectra of the prepared series red $MoSe_2$ samples.

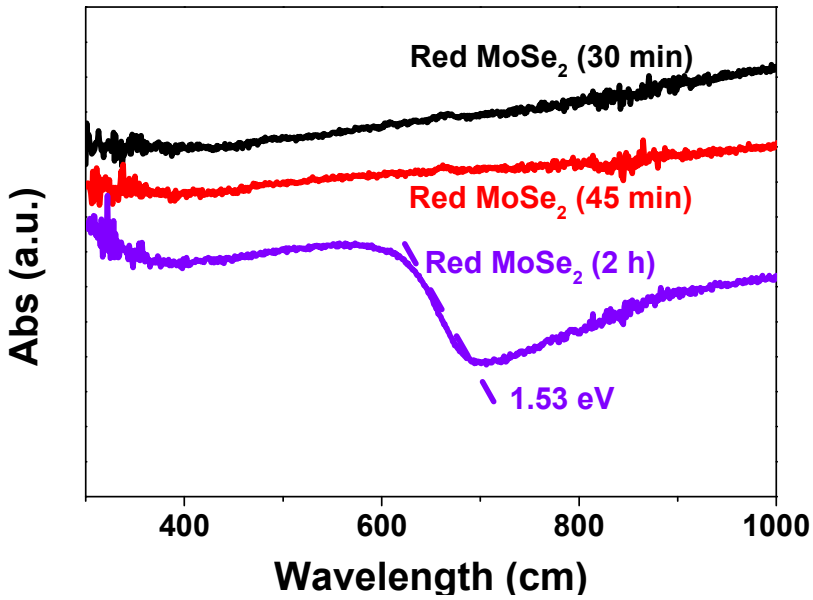

Figure S1. UV–visible absorption spectra showing the different absorption between the prepared series red $MoSe_2$ samples.

UV–visible absorption curves of the series red $MoSe_2$ samples with different annealing time also show dramatical divergence, indicating the evolution on the band gap. After annealing at the oxidized atmosphere about 2h, the red $MoSe_2$ shows a semiconductor characteristic. The bandgap of the red $MoSe_2$ (2h) is estimated to be around 1.53 eV.

3. XRD, SEM and TEM images of the blue MoO_3 nanosheets

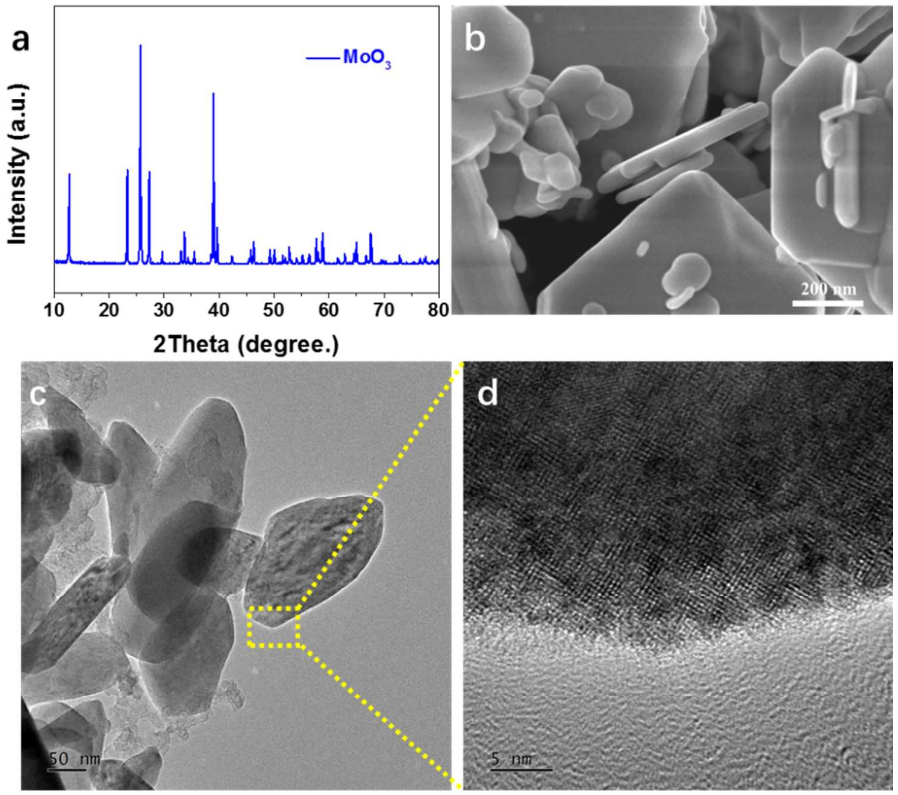

Figure S2. Characterization of blue MoO_3. XRD pattern (a), SEM image (b), TEM and corresponding HRTEM images of the blue MoO_3 nanosheets.

4. SEM and TEM images of the prepared black $MoSe_2$ nanosheets

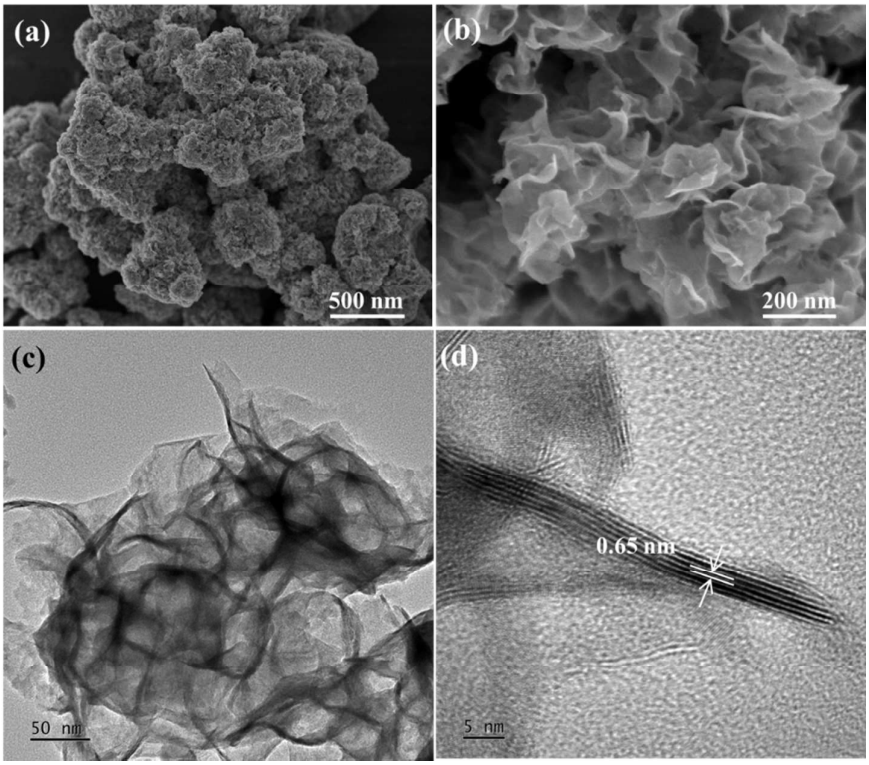

Figure S3. SEM (a) and corresponding enlarged SEM (b) images of the prepared $MoSe_2$ nanosheets. TEM (c) and HRTEM (d) images of the $MoSe_2$ NSs, displaying a uniform d spacing of 0.65 nm for the (002) plane in the $MoSe_2$ NSs.

5. EDX spectra of the red $MoSe_2$ nanosheets

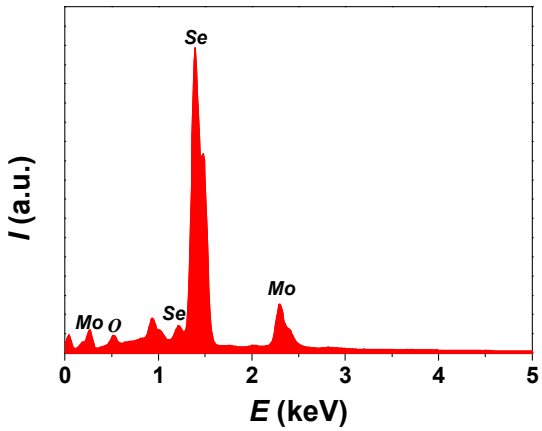

Figure S4. EDS spectra of the red $MoSe_2$ nanosheets, indicating the exist of elements Mo, Se, and O.

6. Elemental mapping images of the red $MoSe_2$ nanosheets.

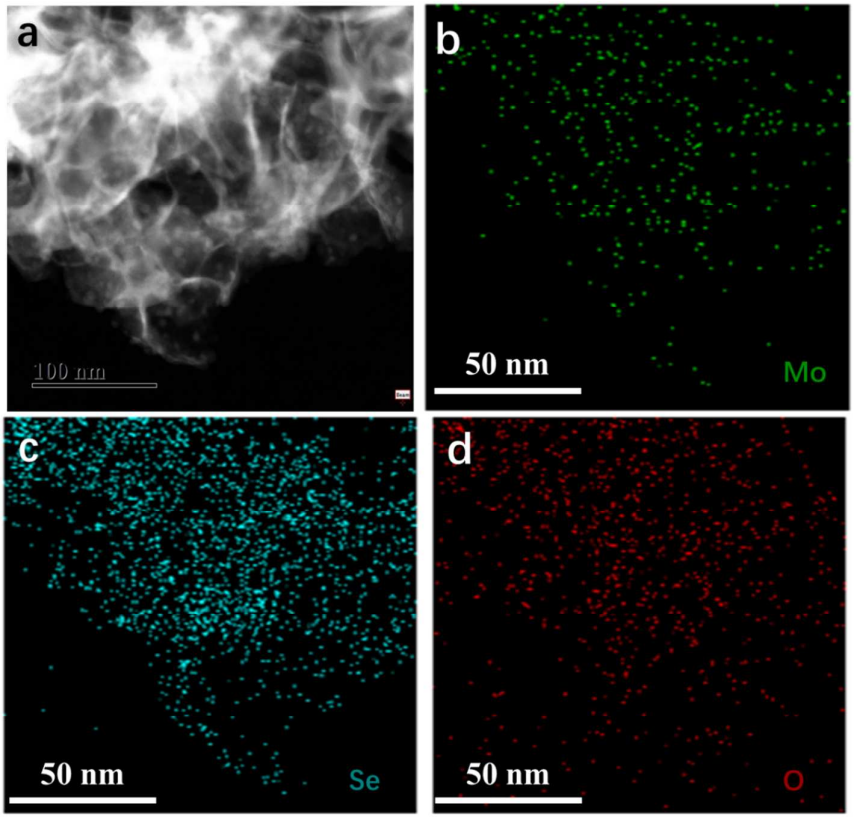

Figure S5. The dark-field TEM images (a) and corresponding element mapping images (b-d) of the prepared red $MoSe_2$ nanosheets (corresponding to area 3 in Figure 2f), suggesting the homogeneous distribution of Mo, O and Se.

7. Conductivity analysis of the prepared series samples.

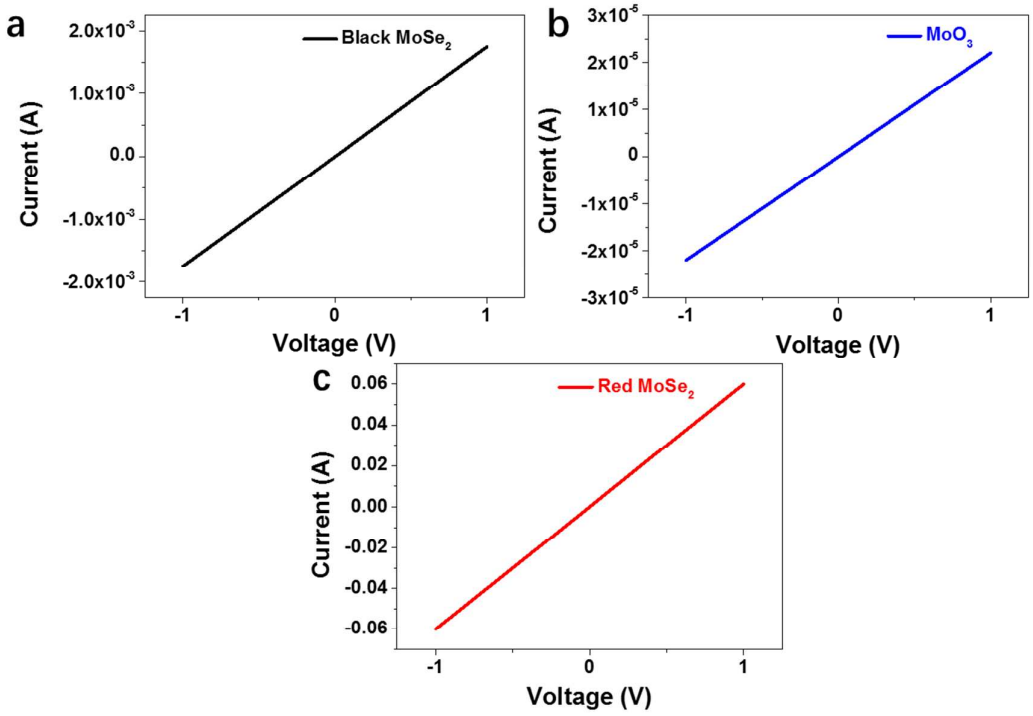

Figure S6. I-V curves of the prepared black $MoSe_2$, red $MoSe_2$ and blue MoO_3.

8. The electronic conductivity of the prepared series red $MoSe_2$ samples.

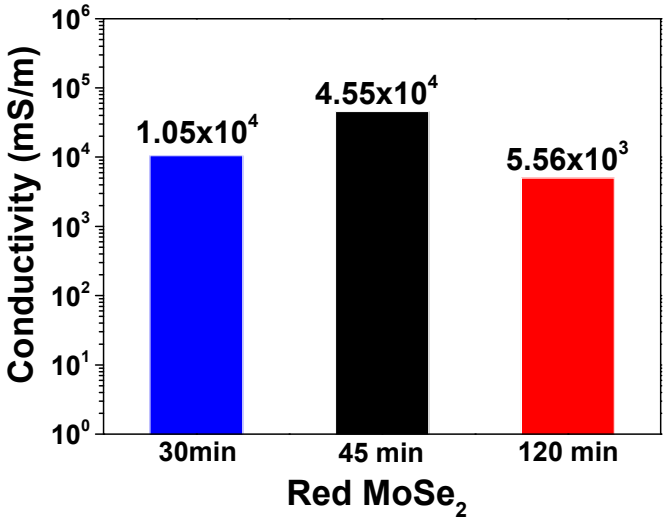

Figure S7. The electronic conductivity of the prepared series red $MoSe_2$ samples.

9. XPS spectra of the red $MoSe_2$ nanosheets.

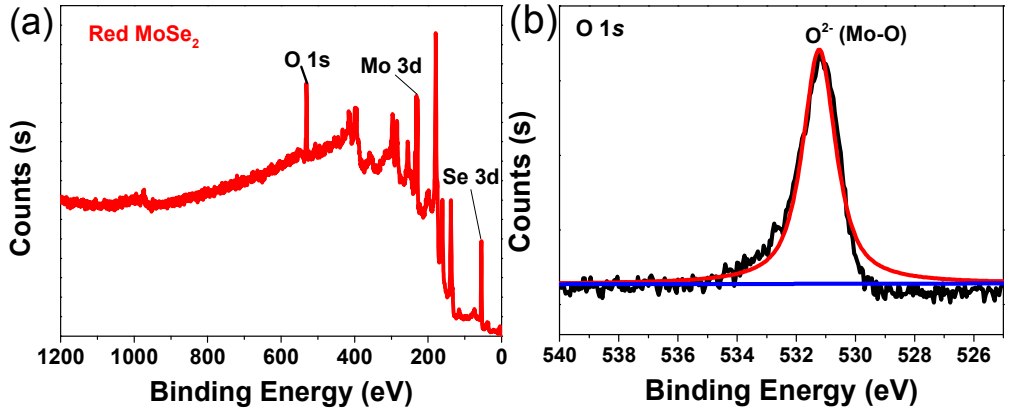

Figure S8. The overall (a) and high resolution O1s XPS spectra (b) of the prepared red $MoSe_2$ nanosheets.

10. XPS spectra of the blue MoO_3 nanosheets.

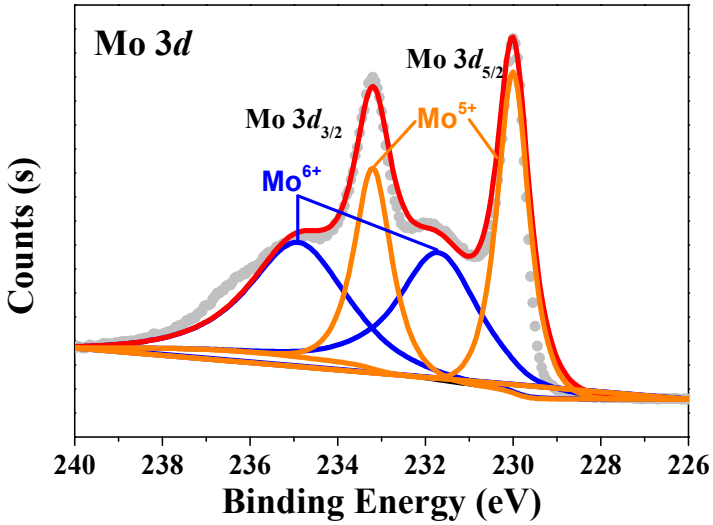

Figure S9. High-resolution XPS spectra of Mo 3d of the blue MoO_3 nanosheets.

The existence of Mo^{5+} verify that the prepared blue MoO_3 nanosheets were not fully oxidized to pure MoO_3 semiconductors

11. BET analysis results of the red $MoSe_2$ nanosheets.

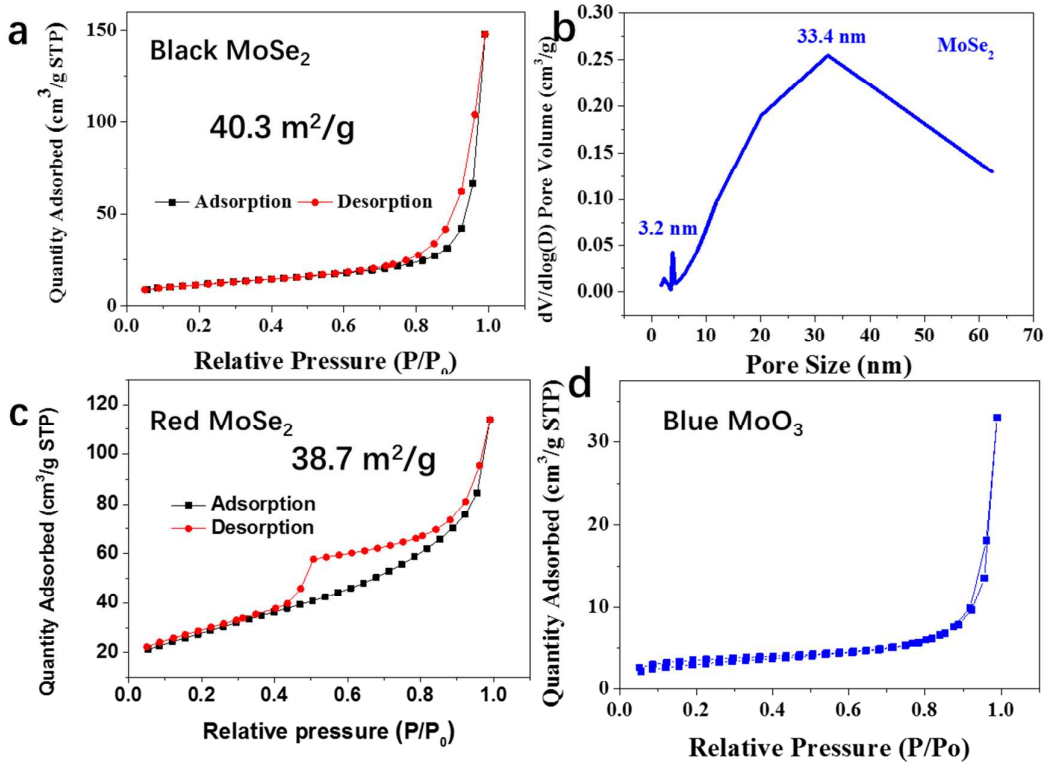

Figure S10 Nitrogen adsorption-desorption isotherms of the prepared black $MoSe_2$ (a), red $MoSe_2$ (c) and blue MoO_3 (d). Corresponding pore size distributions of the prepared black $MoSe_2$ (b).

12. Discharge-charge voltage profiles of the Li-ion batteries with black $MoSe_2$ anode.

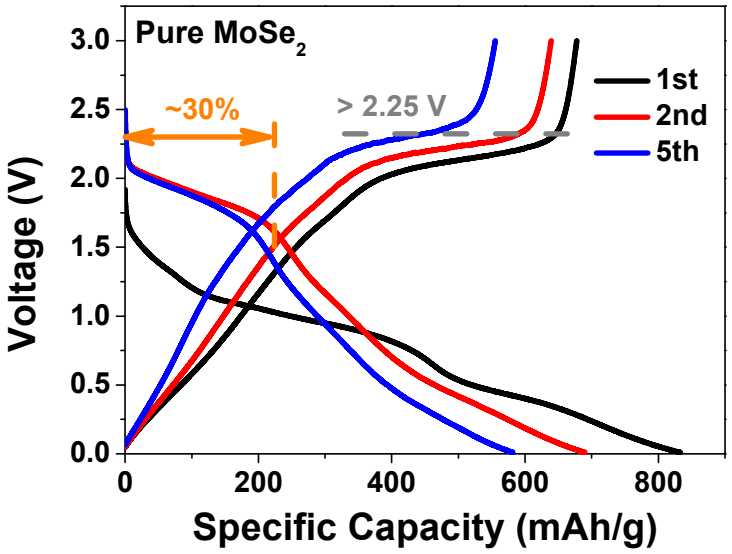

Figure S11. Discharge-charge voltage profiles of prepared black $MoSe_2$ anode in the initial 5 cycles.

13. Discharge-charge voltage profiles of the Li-ion batteries with MoO_3 electrode.

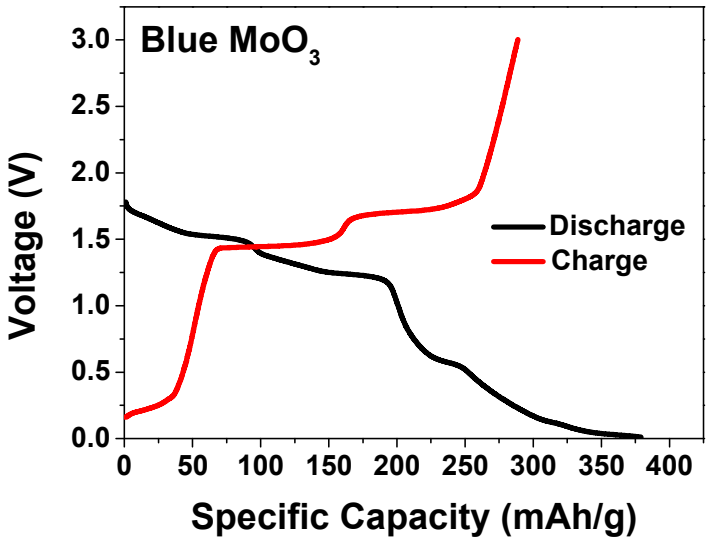

Figure S12. Discharge-charge voltage profiles of prepared blue MoO_3 anode in the initial cycle.

14. CV profiles of red $MoSe_2$ anode

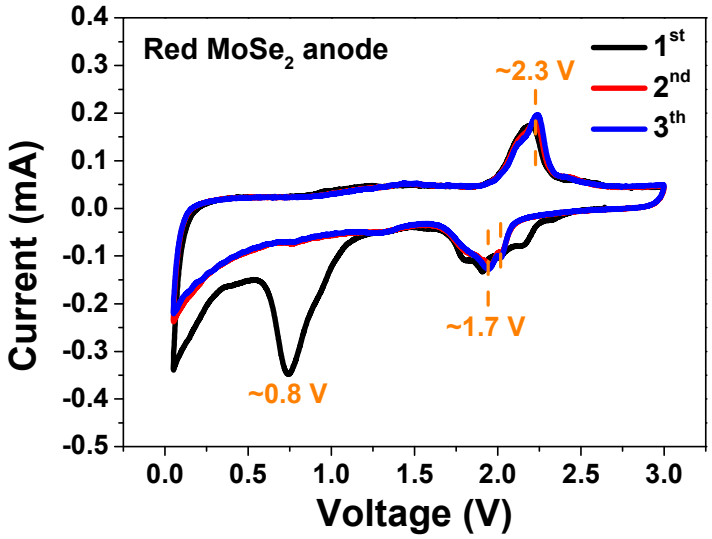

Figure S13. CV profiles of red $MoSe_2$ anode at a scanning rate of 0.1 mV/s showing the 1st, 2nd and 3rd cycles between 0.05 and 3.0 V.

15. Rate capability of the red $MoSe_2$ anode

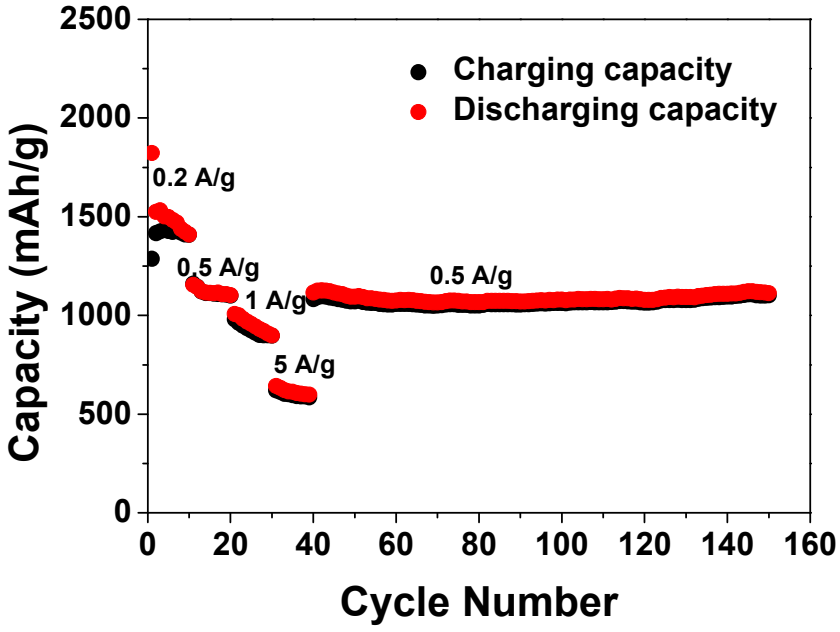

Figure S14. The capacities retention of the red $MoSe_2$ nanosheets, black $MoSe_2$ nanosheets and blue MoO_3 at current densities from 0.2 A g^{-1} to 5 A g^{-1}.